

# COVID-2019 Pneumonia

## Severity and distribution of lung changes observed on the initial chest X-ray as an indicator of final outcomes

\*Rashid S. Al Umairi,<sup>1</sup> Ishaq Al Salmi,<sup>1</sup> Jokha Al Kalbani,<sup>1</sup> Atheel Kamona,<sup>1</sup> Saqar Al Tai,<sup>1</sup> Faiza Al Kindi,<sup>1</sup> Sachin Jose,<sup>2</sup> Faryal Khamis,<sup>3</sup> Huda Al Khalili,<sup>4</sup> Mohammed Al Busaidi<sup>5</sup>

**ABSTRACT: Objectives:** This study aimed to assess the correlation between the severity of the initial chest x-ray (CXR) abnormalities in patients with a confirmed diagnosis of COVID-19 and the final outcomes. **Methods:** This retrospective study was conducted at the Royal Hospital, Oman between mid-March and May 2020 and included patients who had been admitted with a confirmed diagnosis of COVID-19 and had a final outcome. Serial CXRs were identified and examined for presence, extent, distribution and progression pattern of radiological abnormalities. Each lung field was divided into three zones on each CXR and a score was allocated for each zone (0 is normal and 1–4 is mild–severe). The scores for all six zones per CXR examination were summed to provide a cumulative chest radiographic score (range: 0–24). **Results:** A total of 64 patients were included; the majority were male (89.1%) and the mean age was  $50.22 \pm 14.86$  years. The initial CXR was abnormal in 60 patients (93.8%). The most common finding was ground glass opacity ( $n = 58, 96.7\%$ ) followed by consolidation ( $n = 50, 83.3\%$ ). Most patients had bilateral ( $n = 51, 85.0\%$ ), multifocal ( $n = 57, 95.0\%$ ) and mixed central and peripheral ( $n = 36, 60.0\%$ ) lung abnormalities. The median score of initial CXR for deceased patients was significantly higher than recovered patients (17 versus 11;  $P = 0.009$ ). Five CXR evolution patterns were identified: type I (initial radiograph deteriorates then improves), type II (fluctuate), type III (static), type IV (progressive deterioration) and type V (progressive improvement). **Conclusion:** A higher baseline CXR score is associated with higher mortality rate and poor prognosis in those with COVID-19 pneumonia.

**Keywords:** SARS-CoV-2; COVID-19; X-ray Film; Pneumonia; Prognosis; Oman.

### ADVANCES IN KNOWLEDGE

- The findings of this study demonstrate that severe lung abnormalities on chest radiographs are associated with poor clinical outcome prognosis and increased mortality.

### APPLICATION TO PATIENT CARE

- This study highlights the importance of chest radiographs in the initial diagnosis, follow-up and prediction of clinical course/outcome of patients with COVID-19.

IN WUHAN, CHINA IN DECEMBER 2019, SEVERAL cases of severe pneumonia of unknown aetiology were admitted to the hospitals. By January 2020, the cause was identified as a novel coronavirus that was called severe acute respiratory syndrome coronavirus 2 (SARS-CoV-2) by the International Committee on Taxonomy of Viruses on February 22, 2020. The disease was named COVID-19 by the World Health Organisation (WHO) on the same day.<sup>1–3</sup> Since then, the virus has spread worldwide and the WHO classified it as a pandemic on March 11, 2020.<sup>4</sup>

COVID-19 is diagnosed based on the clinical findings and real-time polymerase chain reaction (RT-PCR) assay of specimens obtained from the respiratory tract.<sup>5,6</sup> Medical imaging, including chest computed tomography (CT) and chest x-rays (CXR), plays an important role in its diagnosis and disease progression monitoring upon admission.<sup>7–22</sup>

In the Muscat Governorate of Oman, the Royal Hospital is the main referral hospital for the majority of patients with COVID-19 pneumonia who require admission; CXR is the main imaging modality for diagnosis and follow-up. Quantification of radiographic findings at initial presentation and follow-up can help determine the appropriate management of patients with COVID-19 pneumonia. Therefore, this study aimed to quantify the severity of the CXR findings using a scoring system and to examine the relationship between the severity of the lung changes on the baseline CXR and the final outcomes to determine its prognostic value. Secondly, this study aimed to evaluate the evolution pattern of follow-up CXRs of patients admitted with COVID-19 pneumonia.

## Methods

This retrospective study included all patients with confirmed diagnosis of COVID-19 who were admitted to the Royal Hospital in Muscat, Oman, between mid-March and May 2020 and had a final outcome.

The COVID-19 diagnosis was made based on a positive RT-PCR for SARS-CoV-2 of specimens obtained from the nasopharynx and oropharynx of all patients. Medical records of all patients were reviewed and demographic characteristics, presenting symptoms, vital signs, comorbidities, serum reactive protein, white blood count (WBC) and estimated glomerular filtration rate were obtained. The duration of hospitalisation, admission to the intensive care unit (ICU), history of intubation and the final outcome (death or recovery) were also documented.

All patients had initial frontal CXRs on the day of admission and follow-up CXRs during hospitalisation, obtained in the posteroanterior (PA) projection for those who were able to stand and anteroposterior projection for patients not able to stand. All CXRs were acquired using machines with digital radiography systems using standard techniques (Mobilet Mira Max, Siemens Medical Solution Diagnostic Ltd. Europe, Dublin, Ireland; DRX-Revolution, Carestream Health, Rochester, New York, USA).

Baseline and follow-up CXRs were reviewed retrospectively in consensus by three radiologists with 8–15 years of experience, with all three unaware of final patient outcomes. All CXRs were viewed using a dedicated radiology picture archiving and communication system and were assessed for the presence, distribution and extent of lung abnormalities, including consolidation, ground glass opacity (GGO), cavitation and pleural effusion. Distribution was considered peripheral if the changes were predominantly in the lateral half of the lung fields and central if they were predominantly in the medial half.

For the assessment of the severity of lung changes, each lung field was divided into three equal zones. This was due to technical reasons as most of the CXRs were taken bedside for critically ill patients and it was difficult to identify some anatomical landmarks. Each zone was assigned a score from 0–4 based on the percentage of lung involved (0 = no abnormality, 1 = <25% of the zone involved, 2 = 25–50% involved, 3 = 51–75% involved and 4 = >75% involved). The scores for all six zones of each CXR examination were summed to provide a cumulative chest radiographic score (range, 0–24) [Figure 1]. Evolution patterns of lung changes on serial CXRs were classified into five patterns: I) progression of CXR findings followed

by an improvement; II) fluctuation of CXR findings with at least two CXR peaks and an intervening, mild improvement of more than 25% from the overall mean of CXR scores; III) static CXR findings with no peaks or improvement of more than 25% from the overall mean of CXR scores; IV) progressive deterioration of CXR scores; and V) progressive improvement of CXR scores.

Patients were divided into two groups according to the final outcome: the deceased group and the recovered group. Continuous and discrete data were summarised using the median and interquartile range (IQR). Categorical data were summarised using frequency and percentage. The Chi-squared test (Fisher's exact test/Likelihood Ratio) was used to test the association between the categorical variables. The Mann-Whitney U test was used to compare non-normally distributed continuous and discrete variables. Spearman's rank correlation coefficient was used to assess the correlation between the non-normally distributed continuous variables. Kolmogorov-Smirnov tests were performed to check normal distribution of continuous variables between the groups. Demographic characteristics, CXR scores, comorbidities and other important clinical features were also compared between the groups. A multivariate binary logistic regression analysis was performed to determine the independent predictors of mortality. A *P* value <0.05 was considered statistically significant. All statistical analyses were performed using Statistical Package for the Social Sciences (SPSS), Version 25 (IBM Corp., Chicago, Illinois, USA).

The Scientific Research Committee at the Royal Hospital approved this retrospective, single institution study and waived informed consent (SRC# 59/2020).

## Results

A total of 64 patients were included, 57 men and seven women. The mean age was  $50.22 \pm 14.86$  years. Of those, 29 patients (45.3%) had no comorbidities, 16 patients (25.0%) had a single comorbidity and 19 patients (29.7%) had multiple comorbidities. The duration of hospitalisation ranged between 7–19.5 days with a median of 11.5 days. Of the 64 patients, 44 (68.8%) were admitted to the ICU, 31 (48.4%) required intubation, 17 (26.6%) patients died and 47 (73.4%) recovered. The median duration of ICU admission was 11 days (IQR: 5.3–14.8 days). The median duration of intubation was 10 days (IQR: 7–16.8 days). The fatality rate among patients admitted to the ICU was 38.6% ( $n = 17$ ) [Table 1].

The initial CXRs were acquired at a median of seven days (IQR: 5–8 days) from the onset of

**Table 1:** Characteristics of patients with a confirmed diagnosis of COVID-19 who were admitted to the Royal Hospital, Oman between mid-March and May 2020 (N = 64)

Characteristic	n (%)
<b>Gender</b>	
Male	57 (89.1)
Female	7 (10.9)
<b>Age in years</b>	
Mean ± SD	50.22 ± 14.86
Median (min–max)	46.5 (22–78)
<b>Symptom</b>	
Fever	47 (73.4)
Runny nose	7 (10.9)
Cough	40 (62.5)
SOB	41 (64.1)
Headache	4 (6.3)
Vomiting	1 (1.6)
Nausea	4 (6.3)
Dizziness	1 (1.6)
Muscle ache/body ache	6 (9.4)
Malaise	0 (0)
Lethargy	8 (12.5)
Phalangeal discomfort/pain	11 (17.2)
Chest pain	5 (7.8)
Pleuritic chest pain	1 (1.6)
Abdominal pain	0 (0)
Diarrhoea	12 (18.8)
Haemoptysis	0 (0)
Anorexia	3 (4.7)
<b>Comorbidity</b>	
No comorbidity	29 (45.3)
Single comorbidity	16 (25)
Multiple comorbidity	19 (29.7)
Diabetes mellitus	27 (42.2)
Ischemic heart disease	2 (3.1)
Hyperlipidaemia	5 (7.8)
Chronic kidney disease	6 (9.4)
Hypertension	19 (29.7)
<b>Duration of hospital stay and disease course</b>	
Median days of hospitalisation (IQR)*	11.5 (7.0–19.5)
Number of patients admitted to the ICU	44 (68.8)

Median days of ICU admission (IQR)	11 (5.3–14.8)
Number of patients intubated	31 (48.4)
Median days of intubation (IQR)	10 (7.0–16.8)
<b>Final outcome</b>	
Recovered (i.e. discharged)	47 (73.4)
Deceased	17 (26.6)

\*Hospitalisation duration was from the day of the admission to the day of discharge or death.

SD = standard deviation; SOB = shortness of breath; IQR = interquartile range; ICU = intensive care unit.

**Table 2:** Radiological findings of patients with confirmed diagnosis of COVID-19 included in this study (N = 64)

Finding	n (%)
Abnormal CXR at admission	60 (93.8)
Median days since symptoms started and the CXR was acquired (IQR)	7 (5–8)
<b>Abnormal CXR findings (n = 60)</b>	
Consolidation	50 (83.3)
GGO	58 (96.7)
Cavitation	0 (0)
Central	4 (6.7)
Peripheral	20 (33.3)
Mixed central and peripheral	36 (60.0)
Unilateral	9 (15.0)
Bilateral	51 (85.0)
Unifocal	3 (5.0)
Multifocal	57 (95.0)
Pleural effusion	2 (3.3)
<b>Total score of the baseline CXR</b>	
Mean ± SD	11.91 ± 7.84
Median (IQR)	12.5 (4–18)

CXR = chest x-ray; SD = standard deviation; IQR = interquartile range; GGO = ground glass opacity.

symptoms and were abnormal in 93.8% of the patients (n = 60). The most common finding was GGO (n = 58, 96.7%), followed by consolidation (n = 50, 83.3%). Pleural effusion was a rare finding (n = 2, 3.3%) and none of the patients had cavitation. Bilateral lung involvement (n = 51, 85.0%) was more common than unilateral involvement (n = 9, 15.0%). The right lower (n = 50, 83.3%) and left lower (n = 51, 85.0%) zones were more commonly affected than the right middle (n = 45, 75.0%), left middle (n = 42, 70.0%), right upper (n = 35, 58.3%) and left upper (n = 28, 46.7%) zones. Mixed central and peripheral distribution was the

**Table 3:** Association between Initial Chest X-ray score and patient characteristics

Variable	Total baseline CXR score		P value*
	Median score (IQR)		
<b>Age group in years</b>			
20–29	10 (0.5–19.5)		0.296
30–39	13 (4–16)		
40–49	14 (4–22)		
50–59	7.5 (2.5–11.5)		
60–69	13.5 (6.3–22.8)		
≥70	12 (5–17)		
<b>Diabetes mellitus</b>			
Yes	13 (7–19)		0.149
No	11 (2.5–17.5)		
<b>Hypertension</b>			
Yes	11 (5–18)		0.797
No	13 (4–18.5)		
<b>Ischaemic heart disease</b>			
Yes	6.5 (0–13)		0.288
No	12.5 (4–18.3)		
<b>Chronic kidney disease</b>			
Yes	3.5 (0.8–7.3)		0.010 <sup>†</sup>
No	13 (4.8–19)		
<b>Hyperlipidaemia</b>			
Yes	13 (3–24)		0.625
No	12 (4–18)		
<b>ICU admission</b>			
Yes	14 (12–21)		0.0001 <sup>†</sup>
No	2.5 (1–5)		
<b>Intubation</b>			
Yes	16 (13–21)		0.0001 <sup>†</sup>
No	5 (1.5–12.5)		
<b>Outcome</b>			
Recovered	11 (4–16)		0.009 <sup>†</sup>
Deceased	17 (12–22.5)		

CXR = chest x-ray; IQR = interquartile range; ICU = intensive care unit.

\*Using Mann-Whitney U test.

<sup>†</sup>Statistically significant.

predominant distribution (n = 36, 60.0%), followed by peripheral (n = 20, 33.3%) and central distribution (n = 4, 6.7%). Multifocal distribution was more common (n = 57, 95.0%) than unifocal distribution (n = 3, 5.0%) [Table 2].

**Table 4:** Association between patients' clinical and laboratory findings and final outcome

Variable	Total	n (%)		P value
		Recovered	Deceased	
<b>Gender</b>				
Male	57	42 (73.7)	15 (26.3)	1.000
Female	7	5 (71.4)	2 (28.6)	
Mean age in years ± SD		46.57 ± 13.57	60.29 ± 13.91	0.001*
<b>Diabetes mellitus</b>				
Yes	27	16 (59.3)	11 (40.7)	0.044*
No	37	31 (83.8)	6 (16.2)	
<b>Ischemic heart disease</b>				
Yes	2	2 (100)	0 (0)	1.000
No	62	45 (72.6)	17 (27.4)	
<b>Hyperlipidaemia</b>				
Yes	5	4 (80.0)	1 (20.0)	1.000
No	59	43 (72.9)	16 (27.1)	
<b>Chronic kidney disease</b>				
Yes	6	6 (100)	0 (0)	0.182
No	58	41 (70.7)	17 (29.3)	
<b>Hypertension</b>				
Yes	19	12 (63.2)	7 (36.8)	0.236
No	45	35 (77.8)	10 (22.2)	
<b>WBC count</b>				
Normal	44	36 (81.8)	8 (18.2)	0.034*
Abnormal	20	11 (55.0)	9 (45.0)	
<b>CRP in mg/L</b>				
<10	1	1 (100)	0 (0)	0.137
10–50	15	14 (93.3)	1 (6.7)	
50–100	17	13 (76.5)	4 (23.5)	
100–150	9	6 (66.7)	3 (33.3)	
>150	22	13 (59.1)	9 (40.9)	
<b>Lymphocyte</b>				
Normal	21	16 (76.2)	5 (23.8)	1.000
Abnormal	43	31 (72.1)	12 (27.9)	
<b>Neutrophils</b>				
Normal		22 (84.6)	4 (15.4)	0.149
Abnormal		25 (65.8)	13 (34.2)	

SD = standard deviation; WBC = white blood cell; CRP = C-reactive protein; eGFR = estimate glomerular filtration rate; GGO = ground glass opacity.

\*Statistically significant.

**Table 4 (cont'd.):** Association between patients' clinical and laboratory findings and final outcome

Variable	Total	n (%)		P value
<b>eGFR in mL/min/1.73m<sup>2</sup></b>				
≥90	40	31 (77.5)	9 (22.5)	0.132
60–90	16	11 (68.8)	5 (31.3)	
30–60	4	3 (75.0)	1 (25.0)	
15–30	2	0 (0)	2 (100)	
<15	2	2 (100)	0 (0)	
<b>Consolidation</b>				
Yes	50	34 (68.0)	16 (32.0)	0.089
No	14	13 (92.9)	1 (7.1)	
<b>GGO</b>				
Yes	58	42 (72.4)	16 (27.6)	1.000
No	6	5 (83.3)	1 (16.7)	
<b>Pleural effusion</b>				
Yes	2	1 (50.0)	1 (50.0)	0.464
No	62	46 (74.2)	16 (25.8)	
<b>Progression pattern</b>				
Initial deterioration followed by improvement (type I)	11	9 (81.8)	2 (18.2)	0.014*
Fluctuation (type II)	1	1 (100)	0 (0)	
Static (type III)	18	11 (61.1)	7 (38.9)	
Progressive deterioration (type IV)	12	5 (41.7)	7 (58.3)	
Progressive improvement (type V)	18	17 (94.1)	1 (5.9)	

SD = standard deviation; WBC = white blood cell; CRP = C-reactive protein; eGFR = estimate glomerular filtration rate; GGO = ground glass opacity.

\*Statistically significant.

The median score of initial CXR for deceased patients was significantly higher than for those who recovered (17 versus 11;  $P = 0.009$ ). In addition, there was a higher median score for initial CXRs for those who were admitted to the ICU than those who were not admitted to the ICU (14 versus 2.5;  $P = 0.0001$ ). Similarly, higher median scores of the initial CXRs were observed for those who were intubated compared to those who were not intubated (16 versus 5;  $P = 0.0001$ ) [Table 3].

**Table 5:** Multivariate binary logistic regression analysis to determine the independent predictors of mortality

Variable	B	P value	OR (95% CI)
Age	0.082	0.004*	1.085 (1.027–1.147)
Total baseline CXR score	0.107	0.044*	1.113 (1.003–1.236)
<b>Diabetes mellitus</b>			
No (reference)			
Yes	0.936	0.207	2.550 (0.595–10.928)
<b>WBC count</b>			
Normal (reference)			
Abnormal	1.420	0.065	4.138 (0.916–18.700)

OR = odds ratio; CI = confidence interval; CXR = chest X-ray; WBC = white blood cell.

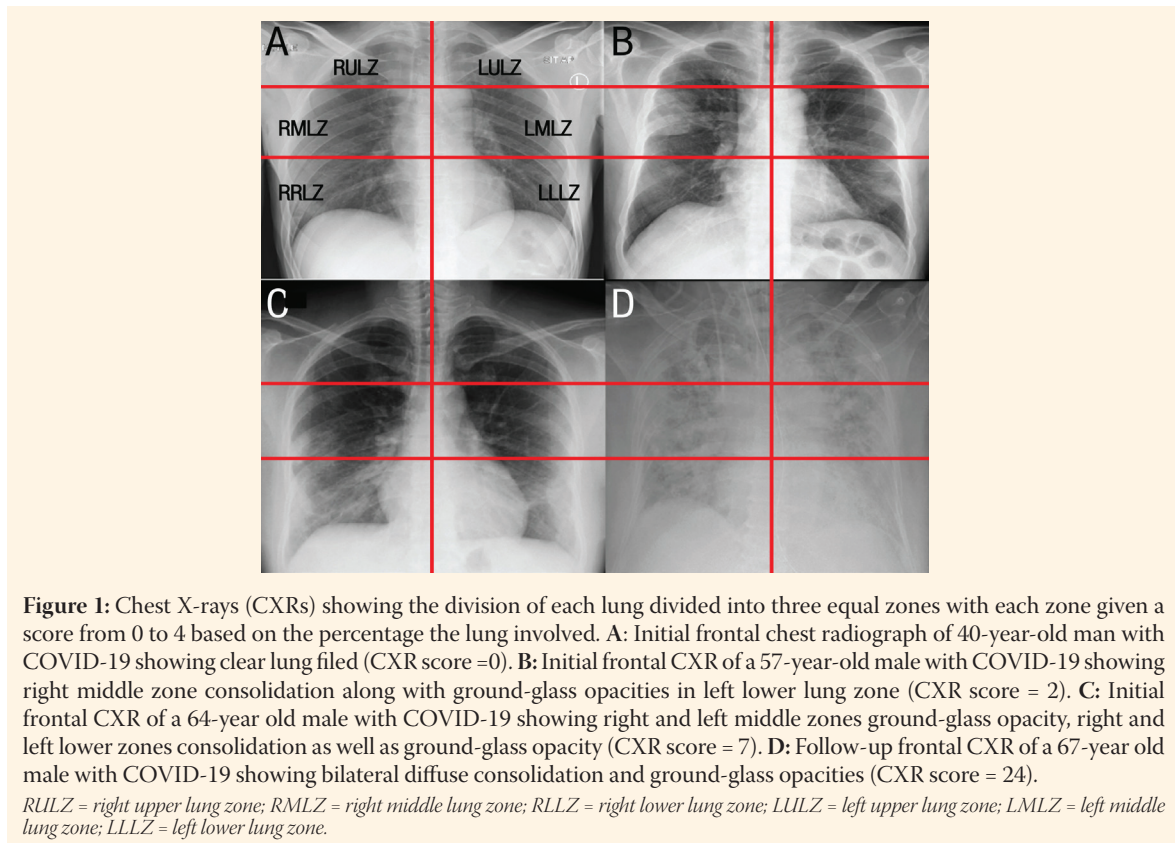
\*Statistically significant.

A significant positive correlation was found between the duration of hospitalisation and the score of the initial CXR (correlation coefficient = 0.381;  $P = 0.002$ ). There was no significant correlation between the initial CXR and duration of ICU admission or intubation.

Upon review of the follow-up CXRs, five evolution patterns were identified: type I (initial deterioration followed by improvement), type II (fluctuate), type III (static), type IV (progressive deterioration) and type V (progressive improvement). Type III and IV progression patterns were the most frequent among the deceased group. Age ( $P = 0.001$ ), diabetes mellitus ( $P = 0.044$ ) and WBC count ( $P = 0.034$ ) were significantly associated with the final outcomes of the patients in the univariate analysis [Table 4].

There was a statistically significant difference in the mortality rate between the comorbidity groups ( $P = 0.004$ ). The mortality rate among patients who had no comorbidity was 10.3% ( $n = 3$ ), whereas the mortality rates among single comorbidity and multiple comorbidity groups were 56.3% ( $n = 9$ ) and 26.3% ( $n = 5$ ), respectively.

A multivariate binary logistic regression was performed to determine the effects of age, baseline CXR score, diabetes mellitus and WBC count on the likelihood of mortality among patients with COVID-19 pneumonia. The logistic regression model was statistically significant ( $\chi^2 [4] = 24.130$ ;  $P = 0.0001$ ). The model explained 45.8% (Nagelkerke  $R^2$ ) of the variance in the outcome mortality and correctly classified 87.5% of cases. Increasing age (odds ratio [OR] = 1.085, 95% confidence interval [CI]: 1.027–1.147;  $P = 0.004$ ) and baseline CXR score (OR = 1.113,



95% CI: 1.003–1.236;  $P = 0.044$ ) were significantly associated with an increased likelihood of mortality [Table 5].

## Discussion

A combination of clinical suspicion, RT-PCR and CXR and CT imaging is used to diagnose COVID-19.<sup>5,23</sup> Although CXR is less sensitive when compared to CT, as well as due to the infection control issues and lack of availability of CT machines in many parts of the world, CXR is an alternative imaging modality that can be used for identification and follow-up of lung abnormalities in patients with COVID-19.<sup>11,24</sup>

In the current study, GGO was the most common CXR manifestation of COVID-19 pneumonia (96.7%), followed by consolidation (83.3%). Mixed peripheral and central distribution of lung abnormalities was the most common distribution (60.0%) followed by peripheral distribution alone (33.3%). Predilection for lower lung zones involvement was another feature of COVID-19 pneumonia on CXR. Pleural effusion was rare as it was seen in only two patients. The absence of cavitation is an important negative finding that, when present, requires consideration of an alternative diagnosis or co-existing or added superinfection. The current study's results are consistent with the findings reported in several recent studies.<sup>11,12</sup>

CXR findings of COVID-19 pneumonia can overlap with other viral pneumonias, in particular, other coronavirus infections, due to the similar pathogenesis of viruses belonging to the same family. For example, SARS and Middle East respiratory syndrome (MERS) share common CXR manifestations with COVID-19.<sup>17</sup> Therefore, these findings need to be interpreted in combination with the clinical context of patients.

The CXR score was found to be an independent predictor of mortality and morbidity of admitted patients with COVID-19 pneumonia in the current study. A higher CXR score is associated with increased duration of hospitalisation, rate of ICU admission and intubation along with increased fatality. Borghesi *et al.* used a different scoring system to quantify the severity of CXR findings of patients with COVID-19 pneumonia. Each CXR was divided into three zones and each zone was given a score as follows: 0 was no lung abnormality, 1 was interstitial infiltrates, 2 was interstitial and alveolar infiltrates (interstitial predominance) and 3 was interstitial and alveolar infiltrates (alveolar predominance). Findings indicated that a high CXR score is associated with higher in-hospital mortality.<sup>25,26</sup>

Regarding the temporal evaluation of lung abnormalities in the current study, progressive deterioration (type IV pattern) and static findings

(type III pattern) were the most common evolution patterns among the deceased group, whereas the progressive improvement pattern was the most frequently observed pattern among recovered patients. Wong *et al.* studied the pattern of progression of 138 patients with SARS and found the most common pattern was initial radiographic deterioration to peak level followed by radiographic improvement.<sup>27</sup> Das *et al.* studied the progression pattern in 55 patients with MERS and found that progressive deterioration was the most common progressive pattern.<sup>28</sup> This study is an adjunct to the current literature since it proposes another quantifying method to assess the severity of CXR findings in patients with COVID-19 that can help stratify patients and plan their management.

Older age and diabetes mellitus were significantly associated with an increased likelihood of mortality. These findings are consistent with results from prior studies.<sup>29</sup>

This study was subject to certain limitations. First, this study had a small sample size. Second, due to this study's retrospective nature, some important clinical information might not be well documented (for example, viral load, oxygen saturation and detailed symptoms at presentation). Lastly, visual estimation of the lung zones and percentage of lung involvement are subjective; therefore, the percentage of lung involvement might be over- or under-estimated.

## Conclusion

A high score of the initial CXR in patients with COVID-19 pneumonia, accompanied by increased age, diabetes mellitus and increased WBC count, were associated with a poor prognosis and higher mortality. This information could help clinicians stratify and manage patients with COVID-19 pneumonia better.

## CONFLICT OF INTEREST

The authors declare no conflicts of interest.

## FUNDING

No funding was received for this study.

## AUTHORS' CONTRIBUTION

RSU and MAB collected the data. RSU, IAS and JAK reviewed the chest X-ray. RSU drafted the manuscript. SJ performed the statistical analysis and wrote the statistical section. AK, SAT, FAK, FK and HAK reviewed the manuscript and provided intellectual input. All authors approved the final version of the manuscript.

## References

1. de Jaegere TMH, Krdzalic J, Fasen BACM, Kwee RM; COVID-19 CT Investigators South-East Netherlands (CISEN) study group. Radiological Society of North America Chest CT Classification System for Reporting COVID-19 Pneumonia: Interobserver Variability and Correlation with Reverse-Transcription Polymerase Chain Reaction. *Radiol Cardiothorac Imaging* 2020; 2:e200213. <https://doi.org/10.1148/ryct.2020200213>.
2. Ge H, Wang X, Yuan X, Xiao G, Wang C, Deng T, et al. The epidemiology and clinical information about COVID-19. *Eur J Clin Microbiol Infect Dis* 2020; 39:1011–19. <https://doi.org/10.1007/s10096-020-03874-z>.
3. Chen N, Zhou M, Dong X, Qu J, Gong F, Han Y, et al. Epidemiological and clinical characteristics of 99 cases of 2019 novel coronavirus pneumonia in Wuhan, China: A descriptive study. *Lancet* 2020; 395:507–13. [https://doi.org/10.1016/s0140-6736\(20\)30211-7](https://doi.org/10.1016/s0140-6736(20)30211-7).
4. World Health Organization. Coronavirus disease 2019 events as they happen 2020. From: <https://www.who.int/emergencies/diseases/novel-coronavirus-2019/events-as-they-happen> Accessed: Dec 2020.
5. Udugama B, Kadhiresan P, Kozlowski HN, Malekjahani A, Osborne M, Li VYC, et al. Diagnosing COVID-19: The disease and tools for detection. *ACS Nano* 2020; 14:3822–35. <https://doi.org/10.1021/acsnano.0c02624>.
6. Rothan HA, Byrareddy SN. The epidemiology and pathogenesis of coronavirus disease (COVID-19) outbreak. *J Autoimmun* 2020; 109:102433. <https://doi.org/10.1016/j.jaut.2020.102433>.
7. Ai T, Yang Z, Hou H, Zhan C, Chen C, Lv W, et al. Correlation of chest CT and RT-PCR testing for coronavirus disease 2019 (COVID-19) in China: A report of 1014 cases. *Radiology* 2020; 296:E32–40. <https://doi.org/10.1148/radiol.2020200642>.
8. Liu J, Yu H, Zhang S. The indispensable role of chest CT in the detection of coronavirus disease 2019 (COVID-19). *Eur J Nucl Med Mol Imaging* 2020; 47:1638–9. <https://doi.org/10.1007/s00259-020-04795-x>.
9. Bai HX, Hsieh B, Xiong Z, Halsey K, Choi JW, Tran TML, et al. Performance of radiologists in differentiating COVID-19 from non-COVID-19 viral pneumonia at chest CT. *Radiology* 2020; 296:E46–54. <https://doi.org/10.1148/radiol.2020200823>.
10. Fang Y, Zhang H, Xie J, Lin M, Ying L, Pang P, et al. Sensitivity of chest CT for COVID-19: Comparison to RT-PCR. *Radiology* 2020; 296:E115–17. <https://doi.org/10.1148/radiol.2020200432>.
11. Wong HYE, Lam HYS, Fong AH, Leung ST, Chin TW, Lo CSY, et al. Frequency and distribution of chest radiographic findings in patients positive for COVID-19. *Radiology* 2020; 296:E78–8. <https://doi.org/10.1148/radiol.2020201160>.
12. Lomoro P, Verde F, Zerboni F, Simonetti I, Borghi C, Fachinetti C, et al. COVID-19 pneumonia manifestations at the admission on chest ultrasound, radiographs, and CT: Single-center study and comprehensive radiologic literature review. *Eur J Radiol Open* 2020; 7:100231. <https://doi.org/10.1016/j.ejro.2020.100231>.
13. Cheng Z, Lu Y, Cao Q, Qin L, Pan Z, Yan F, et al. Clinical features and chest CT manifestations of coronavirus disease 2019 (COVID-19) in a single-center study in Shanghai, China. *AJR Am J Roentgenol* 2020; 215:121–6. <https://doi.org/10.2214/ajr.20.22959>.
14. Chung M, Bernheim A, Mei X, Zhang N, Huang M, Zeng X, et al. CT imaging features of 2019 novel coronavirus (2019-nCoV). *Radiology* 2020; 295:202–7. <https://doi.org/10.1148/radiol.2020200230>.
15. Han R, Huang L, Jiang H, Dong J, Peng H, Zhang D. Early clinical and CT manifestations of coronavirus disease 2019 (COVID-19) pneumonia. *AJR Am J Roentgenol* 2020; 215:338–43. <https://doi.org/10.2214/ajr.20.22961>.

16. Li K, Wu J, Wu F, Guo D, Chen L, Fang Z, et al. The clinical and chest CT features associated with severe and critical COVID-19 pneumonia. *Invest Radiol* 2020; 55:327–31. <https://doi.org/10.1097/RLI.0000000000000672>.
17. Li Y, Xia L. Coronavirus disease 2019 (COVID-19): Role of chest CT in diagnosis and management. *AJR Am J Roentgenol* 2020; 214:1280–6. <https://doi.org/10.2214/ajr.20.22954>.
18. Ng MY, Lee EYP, Yang J, Yang F, Li X, Wang H, et al. Imaging profile of the COVID-19 infection: Radiologic findings and literature review. *Radiol Cardiothorac Imaging* 2020; 2:e200034. <https://doi.org/10.1148/ryct.2020200034>.
19. Wu J, Wu X, Zeng W, Guo D, Fang Z, Chen L, et al. Chest CT findings in patients with coronavirus disease 2019 and its relationship with clinical features. *Invest Radiol* 2020; 55:257–61. <https://doi.org/10.1097/rli.0000000000000670>.
20. Xiong Y, Sun D, Liu Y, Fan Y, Zhao L, Li X, et al. Clinical and high-resolution CT features of the COVID-19 infection: Comparison of the initial and follow-up changes. *Invest Radiol* 2020; 55:332–9. <https://doi.org/10.1097/rli.0000000000000674>.
21. Xu X, Yu C, Qu J, Zhang L, Jiang S, Huang D, et al. Imaging and clinical features of patients with 2019 novel coronavirus SARS-CoV-2. *Eur J Nucl Med Mol Imaging* 2020; 47:1275–80. <https://doi.org/10.1007/s00259-020-04735-9>.
22. Xu YH, Dong JH, An WM, Lv XY, Yin XP, Zhang JZ, et al. Clinical and computed tomographic imaging features of novel coronavirus pneumonia caused by SARS-CoV-2. *J Infect* 2020; 80:394–400. <https://doi.org/10.1016/j.jinf.2020.02.017>.
23. Singhal T. A review of coronavirus disease-2019 (COVID-19). *Indian J Pediatr* 2020; 87:281–6. <https://doi.org/10.1007/s12098-020-03263-6>.
24. American College of Radiology. ACR recommendations for the use of chest radiography and computed tomography (CT) for suspected COVID-19 infection. From: <https://www.acr.org/Advocacy-and-Economics/ACR-Position-Statements/Recommendations-for-Chest-Radiography-and-CT-for-Suspected-COVID19-Infection> Accessed: Dec 2020.
25. Borghesi A, Zigliani A, Golemi S, Carapella N, Maculotti P, Farina D, et al. Chest X-ray severity index as a predictor of in-hospital mortality in coronavirus disease 2019: A study of 302 patients from Italy. *Int J Infect Dis* 2020; 96:291–3. <https://doi.org/10.1016/j.ijid.2020.05.021>.
26. Borghesi A, Maroldi R. COVID-19 outbreak in Italy: Experimental chest X-ray scoring system for quantifying and monitoring disease progression. *Radiol Med* 2020; 125:509–13. <https://doi.org/10.1007/s11547-020-01200-3>.
27. Wong KT, Antonio GE, Hui DS, Lee N, Yuen EH, Wu A, et al. Severe acute respiratory syndrome: Radiographic appearances and pattern of progression in 138 patients. *Radiology* 2003; 228:401–6. <https://doi.org/10.1148/radiol.2282030593>.
28. Das KM, Lee EY, Al Jawder SE, Enani MA, Singh R, Skakni L, et al. Acute Middle East respiratory syndrome coronavirus: Temporal lung changes observed on the chest radiographs of 55 patients. *AJR Am J Roentgenol* 2015; 205:W267–74. <https://doi.org/10.2214/ajr.15.14445>.
29. Lu L, Zhong W, Bian Z, Li Z, Zhang K, Liang B, et al. A comparison of mortality-related risk factors of COVID-19, SARS, and MERS: A systematic review and meta-analysis. *J Infect* 2020; 81:e18–25. <https://doi.org/10.1016/j.jinf.2020.07.002>.